Research paper

Available Online at http://www.recentscientific.com

CODEN: IJRSFP (USA)

International Journal of Recent Scientific Research

International Journal of Recent Scientific Research
Vol. 17, Issue, 06, pp.722-727, June 2026

ISSN: 0976-3031

Subject Area : Physics

SYNTHESIS AND CHARACTERIZATION OF $MgMn_2O_4$ NANORODS FOR SUPERCAPACITOR ELECTRODE APPLICATIONS

P. Vijayamathubalan[1], S. Sivaraj[2], R. Gunaseelan[2], V. Venkatachalam[3], P. Sutharsan[3], S. Abraham Rajasekar[3]* and S. Selvakumar[1]

[1]PG and Research Department of Physics, Government Arts College (Autonomous), Chennai 600 035, Tamil Nadu, India.
[2]Department of Physics, Pachaiyappa's College for Men, Kanchipuram, 631 501, Tamil Nadu, India
[3]Department of Physics, Sir Theagaraya College, Old Washermanpet, Chennai 600 021, Tamil Nadu, India

DOI: http://dx.doi.org/10.24327/ijrsr.20261706.0132

ARTICLE INFO

Article History:

Received 15th May 2026
Received in revised form 28th May2026
Accepted 18th June 2026
Published online 28th June 2026

Key words:

$MgMn_2O_4$ nanorods; XRD; SEM; EDS; Dunn's method; Energy storage.

ABSTRACT

In the present work, $MgMn_2O_4$ energy storage nanomaterials were prepared by the co-precipitation technique and reported. $MgMn_2O_4$ was comprehensively characterized using a variety of analytical techniques to obtain a better understanding of its physicochemical properties. These techniques included powder X-ray diffraction (XRD) for phase identification and crystal structure analysis, Fourier-transform infrared (FTIR) spectroscopy for functional group identification, scanning electron microscopy (SEM) for morphological analysis, and energy-dispersive spectroscopy (EDS) for elemental analysis. Cyclic voltammetry (CV) analysis showed that $MgMn_2O_4$ electrodes exhibit 355 F g^{-1} at a scan rate of 5 mV/s in 6 M KOH electrolyte solution. A detailed understanding of the structural, chemical, and morphological properties of $MgMn_2O_4$ provides valuable insights into its potential use as an electrode component for supercapacitors.

INTRODUCTION

One of the hardest and most difficult tasks of the twenty-first century is to satisfy an increasing need for sustainable, clean, and renewable energy. The main obstacle to the utilization of renewable energy sources such as wind and solar is the insufficient strength, non-availability and ineffective of the acquired electricity due to the fact sunlight can be available during the day but not at night, as well as the wind never blew on our needs. In addition, the rapid increase in environmental pollution, the rise in petroleum prices, the effects of global warming, and the harmful impacts of fossil fuels are compelling researchers to create a revolutionary energy storage material and establish a renewable and environmentally friendly energy storage device that offers a continuous power supply[1–3]. Even though, lithium-ion batteries play an important role in the world of energy industries because of their high energy density. The reversible ion adsorption process of supercapacitors makes them most suitable for applications requiring a high power density. When compared to batteries, supercapacitors have superior properties that include extended life over Portable and smart electronic devices, efficiencies in the manufacturing process, and almost no explosion risk.

Supercapacitors are categorized as either electrochemical double-layer capacitors (EDLC) or pseudocapacitors (PC) on the basis of their charge storage mechanisms.In the EDLC storage mechanism, the electrolyte ions interact electrostatically with the electrode surface. The EDLC mechanism occurs mainly in carbon-based materials like graphene, carbon nanotubes, and activated carbon fiber. In the PC storage process, the electrode and electrolyte undergo reversible faradaic reactions. Materials such as conducting polymers, chalcogenides, metal oxides,and transition metal oxides can be expressing the storage behaviour of PCs [4–5]. EDLC materials possessed a wide range of beneficial properties including high surface area, high power output, excellent durability, long lifespan, and higher electrical conductivity. But unfortunately, the low specific capacitance of EDLCs restricts their high energy density. Moreover, Psedocapacitors are appropriate for supercapacitors due to their large specific capacitance as well as their high energy density.

*Corresponding author: **Dr. S. Abraham Rajasekar**

Associate Professor, Department of Physics,
Sir Theagaraya College, Old Washermanpet, Chennai 600 021, Tamil Nadu, India

There are several factors that influence supercapacitor performance such as the shape and dimensions of the particles, the size of both particles and grains, chemical composition and the porosity and pore size distribution of the prepared electrode material. Nanotechnology can significantly enhance these properties in electrode materials, which helps them store more energy.Researchers have looked into a variety of materials as prospective electrodes for energy storage devices, among them transition-based metal oxides offer a wide variety of materials with excellent capacitance and electrochemical characteristics such as NiO [6], ZnO [7], WO_3 [8], CuO [9], ZrO_2 [10]. However, their short cycle life, low conductivity, and low stability make them not suitable for practical use. As a result, current trends are focused on spinel-based binary and mixed transition metal oxides, because of their improved cycle life, capacitance stability, increased electronic conductivity, and multi-oxidation states, making them the best choice for supercapacitor applications.

The spinel structure of AB_2O_4 appears in the binary transition metal oxides. The spinel structure is made up of A and B metal atoms, and oxygen atoms. The A metal atoms fit into tetrahedral sites, while the B metal atoms fit into octahedral sites in the crystal lattice. The oxygen atoms form a face-centered cubic close-packed arrangement. The excellent symmetry of the spinel structure delivers uniform distribution of metal ions and oxygen vacancies throughout the crystal also enhancing charge transfer and storage. Many studies have been conducted to determine the potential and the performance of binary transition metal oxides for supercapacitors, such as $NiFe_2O_4$[11], $CoFe_2O_4$ [12], and $NiCo_2O_4$ [13]. In recent times the manganese(Mn) spinel material has also been explored for use in supercapacitors. The Mn-spinel structure contains Mn_3O_4 as the parent composition. Many types of metal cations such as cobalt (Co), nickel (Ni), magnesium (Mg), and zinc (Zn) can be inserted into the structure in tetrahedral or octahedral places The electronic conductivity in these oxides takes place through the transfer of charged particles between metal cations of different oxidation states. By replacing one mole of manganese (Mn) cations in Mn_3O_4, the conductivity of the oxide can be improved.The metal oxides composed of two different types of metal cations exhibit better electrochemical performance compared to oxides made of only one type of metal cation. Therefore, adding Co, Ni, Mg, and Zn cations to Mn_3O_4 can improve its capacitive performance. However, the research on $MgMn_2O_4$ is quite limited. For example, Jai Bhagwan et al. reported Spinel-$MgMn_2O_4$ nanofibers with a specific capacitance of 345 F g-1 in 1 M H_2SO_4 electrolyte solution [14]. However, the electrochemical characteristics of $MgMn_2O_4$ can be enhanced for better performance through an inexpensive preparation process.

In this study, $MgMn_2O_4$ nano-rods were synthesized using a co-precipitation technique with dual hydroxides (KOH+NaOH), and their effectiveness in supercapacitor applications was evaluated. The electrochemical characterization of the prepared electrode was examined by Cyclic voltammetry in a 6 M KOH electrolyte solution. Finally, the electrochemical results of the electrode were compared with earlier studies to understand the material well.

EXPERIMENTAL SECTION

Material Synthesis

To create the solution, $MgCl_2$•$2H_2O$ (1 g) and $MnCl_2.4H_2O$ (2 g) were blended in 50 ml double distilled water and magnetically mixed over half an hour to create solution A. Simultaneously, solution B was made by dissolve the NaOH (1 g) and KOH (1 g) in 50 ml double distilled water and mixed well over same half an hour. The colorless solution B was gradually added to Solution A in a dropwise manner. The solution stirred for 6 hours until a light brownishcolour was form. After settling at the base of the beaker, the brown residue was collected and washed multiple times with double distilled water and ethanol. Lastly, it was subjected to overnight drying in a hot air oven set at 100° C. After drying the sample, it was crushed into a fine powder with a mortar, and post-calcinated for 5 hours at 450° C.

Characterization of $MgMn_2O_4$ material

Powder X-ray diffraction (PXRD) identified the crystal structure on a Bruker D8 Advance diffractometer using CuK radiation. Fourier-transform infrared (FTIR) spectroscopy was performed using a Perkin Elmer Spectrum Two spectrometer analyzer to analyse the molecular vibrations material.The Emcraft Genesis 1100 was utilised to capture a morphological image of the surface and texture. Energy-dispersive X-ray spectroscopy (EDS) was employed to investigate the elemental compositions using a BRUKER nano GmbH D-12489 (Germany) equipment. Finally, electrochemical methodology was used to investigate the electrochemical features of the material using an SAS OrigalysElectrochem workstation.

Fabrication of working electrode and electrochemical test

The electrochemical properties of $MgMn_2O_4$ nano-rods were evaluated using Cyclic voltammetry. Graphite paper was utilised as the current collector to make a working electrode. The graphite paper was washed using double distilled water and acetone. The electrode slurry was created by dissolving the active material, conducting agent, and binding agent in N-methyl-2-pyrrolidone in an 80:10:10 ratio (in weight percentage). Afterwards, the electrode slurry was applied on graphite paper. Electrochemical analysis was done with a three-electrode system. The counter electrodes were made of platinum wire, reference electrodes from Ag/AgCl, and working electrodes from graphite paper coated with $MgMn_2O_4$.The CV measurements were performed in different scanning rates from 5 mVs^{-1} to 100 mVs^{-1} at 0.0 to 0.5 V potential window. The specific capacitance values of the synthesised$MgMn_2O_4$ electrode were determined using CV methods.

RESULTS AND DISCUSSION

Powder X-ray diffraction studies (PXRD)

A powder XRD was utilized to examine the phase composition and crystal structure of $MgMn_2O_4$. A diffraction pattern for the material is shown in Fig. 1. The diffraction pattern closely resembled with the standard JCPDS card # 01-072-1336, which suggests that $MgMn_2O_4$ has a cubic structure and belongs to the Fd3m space group. Diffraction pattern with strong peaks indicate high crystalline order, while weak peaks indicate smaller grains. The high degree of crystalline structure and the complete absence of impurities indicates that the material is

strong and stable, which ensures reliable performance in electrochemical processes. The main peaks observed in the powder XRD pattern were located at 18.18°, 29.24°, 31.21°, 32.87°, 36.35°, 36.85°, 38.76°, 44.72°, 51.71°, 54.33°, 56.60°, 58.94°, 60.64°, 64.40°, 65.09°, 74.87°, 77.21° and 78.41°, which are attributed to the crystal planes (101), (112), (200), (103), (211), (202), (004), (220), (105), (312), (303), (321), (224), (116), (400), (413), (422) and (404) of the $MgMn_2O_4$ spinel. To determine the average crystallite size of the $MgMn_2O_4$ sample, the Debye-Scherer formula was applied.

$$\text{Average crystallite size} = \frac{K\times\lambda}{\beta cos\theta} \text{ --------- (1)}$$

Where K denotes the shape coefficient, λ indicates the X-ray wavelength produced by the source, θ represents the Bragg angle, and β corresponds to the full-width at half maximum (FWHM) of the diffraction peak. Based on the calculations, the average crystallite size was around 37.91 nm. The smaller crystalline size would be advantageous in supercapacitors because it might offer more surface area, leading to higher specific capacitance and more efficient electrochemical reactions. Also, The dislocation density ($\delta=1/D^2$) was determined to identify crystal flaws or irregularities. The value of dislocation density determined and measured to be 1.6112×10^{15}. Additionally, the micro-strain value of $MgMn_2O_4$ was determined by applying the following formula:

$$\text{Micro-strain } (\varepsilon) = \frac{\beta cos\theta}{4} \text{--------- (2)}$$

The value of ε was found and acquired to be 0.00297. The micro-stress (σ) can be determined using Hooke's law (σ = Cε) based on the calculated micro-strain value, where C represents the bulk Young's modulus with a value of 1.46 ± 10^{10} N/m2. The micro-stress was calculated to be a 43.4772 M Pa. The lower dislocation density as well as the micro-strain value assure excellent mechanical stability, which upholds the long-lasting reliability of $MgMn_2O_4$. Micro-stress also signifies strong mechanical strength and the capacity to endure external stress in real-world applications.

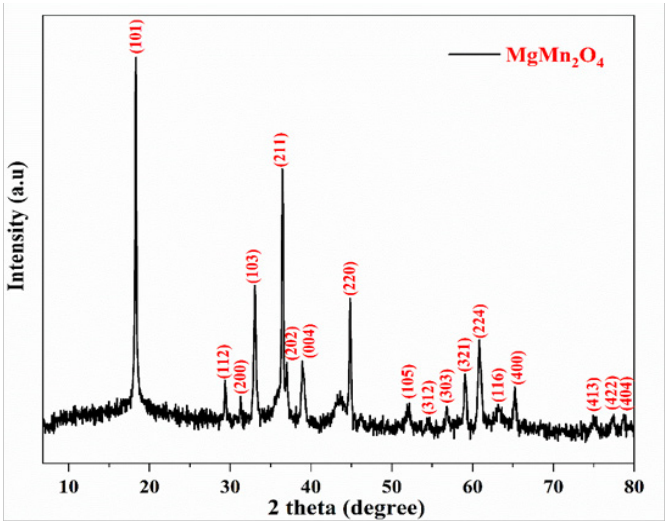

Fig. 1.Powder XRD analysis of $MgMn_2O_4$ nano-rods

Fourier transform infrared spectroscopy analysis (FTIR)

The Fourier-transform infrared (FTIR) spectrum provides valuable information about the functional groups contained in $MgMn_2O_4$ nanorods, as illustrated in Fig. 2. The broad absorption peak observed at 3436.45 cm^{-1} is due to the O-H vibration absorbed by the sample. The peak present at 1640.76 cm-1 is attributed to the existence of a carbonyl (C=O) functional group in the sample. Additionally, two more peaks were seen at 1417.67 cm^{-1} and 1272.04 cm^{-1}, corresponding to CH_2 group movements in a scissoring and wagging pattern. The presence of tetrahedral and octahedral of Mg-O, Mn-O vibrational modes can be determined from the observed peaks at 499 cm^{-1} and 656 cm^{-1}, respectively. These peaks show that the Mg-Mn-O bonding exists in the sample. The existence of the Mg-Mn-O bond, combined with the presence of multiple functional groups, can significantly improve the electrochemical properties of the $MgMn_2O_4$ in the supercapacitor. This functional groups create reactive sites on the surface of the material, while the Mg-Mn-O bond can increase their conductivity also stability. The overall effect of these features is to increase the capacity and durability of the supercapacitor, making the material a promising candidate for energy storage applications. Hence, the results obtained from the FTIR indicate that $MgMn_2O_4$ is a suitable material for usage in supercapacitors.

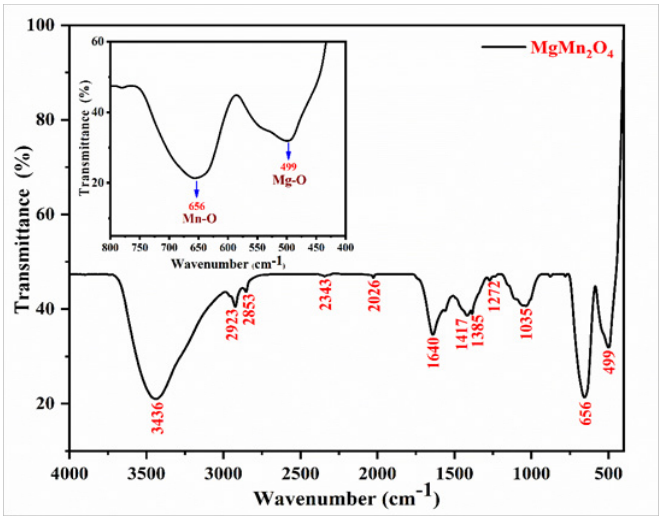

Fig. 2. The IR spectrum analysis of $MgMn_2O_4$ nanorods. (Inset:Metallic-Oxygen Vibrations within the Wavenumber Range of 400-800 cm^{-1})

Morphological studies

The morphology of $MgMn_2O_4$ material was analyzed using SEM with 100 nm resolution to understand its suitability in supercapacitors. The observed SEM images of $MgMn_2O_4$ synthesized from dual hydroxide treatment revealed a nano-rod shape with some agglomerates, as exhibited in Fig. 3 (a), and the related statistical histogram graph given in Fig. 3 (b). The agglomeration in the nano-rods is attributed to surface tension between the particle created on $MgMn_2O_4$. The statistical histogram indicated that the majority of the particles in $MgMn_2O_4$ sample have sizes ranging from 40 to 50 nm. This nanoscale range is ideal in supercapacitor applications because it maximises the surface area of a $MgMn_2O_4$ electrode and facilitates excessive electrolyte ions were absorbed on the surface of an electrode. As a result, the capacitance increases. Additionally, the nano-rod shape allows for strong retention of electrolyte ions. The distinctive structure of $MgMn_2O_4$ improves the far-

adaic effect, resulting in strong electrochemical activity and effective charge storage. These findings indicate that the synthesized $MgMn_2O_4$ sample has remarkable use for supercapacitors.

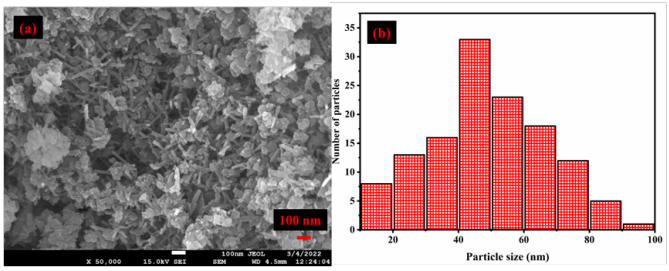

Fig. 3. (a) $MgMn_2O_4$ surface morphology at 100 nm(b)size distribution through Statistical Histogram

Energy-dispersive X-ray spectroscopy (EDS)

EDS analysis was conducted to examine the elemental content and the occupancy ratio of the $MgMn_2O_4$ materials. The existence of Mg, Mn, and O elements was confirmed by the EDS spectrum in Fig. 4, and their respective atomic percentage were identified to be 22.20%, 18.86%, and 64.94%, which is almost near the value of the original stoichiometry. This shows that the produced $MgMn_2O_4$ was highly pure and free of any secondary phases or impurities. The powder XRD analysis also revealed the pure phase formation of $MgMn_2O_4$, similar to the EDS observation. The excellent purity of the prepared $MgMn_2O_4$ is important consideration for its prospective usage in supercapacitors. Negative electrochemical effects can be avoided by using materials free of impurities and secondary phases. Based on the EDS results, the synthesised $MgMn_2O_4$ can also be further examined for their electrochemical characteristics for supercapacitor applications.

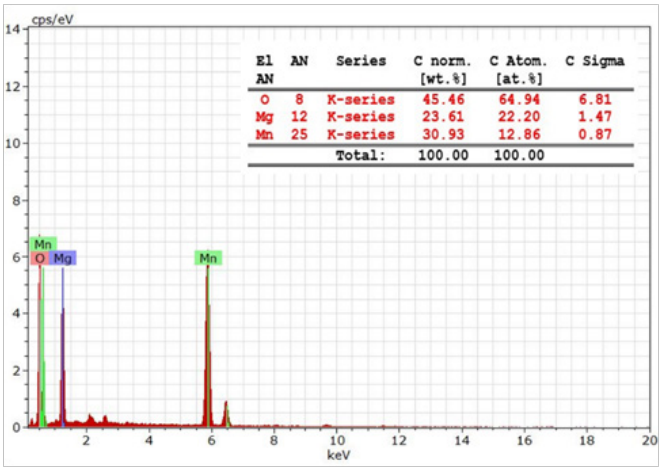

Fig. 4. The Spectrum of Energy-Dispersive X-ray analysis for $MgMn_2O_4$

ELECTROCHEMICAL STUDIES

Cyclic voltammetry analysis

Cyclic voltammetry (CV) test was performed to obtain the charge-storage ability and the energy storing mechanism of a $MgMn_2O_4$ electrode. Fig. 5. (a) shows the CV curves for the $MgMn_2O_4$ electrode in 6 M KOH electrolytes at various scan rates ranging from 0.0 to 0.5 V. The electrode demonstrated excellent electrochemical reversibility and capability, as seen by the continuous symmetry of the CV curves across multiple scan rates. The obtained CV curves confirm the pseudo-capacitive behavior of the material and provide evidence for the faradic redox mechanism. The formula used to calculate the specific capacitance of the $MgMn_2O_4$ electrode was derived from the CV curves, as follows:

$$C_s = \frac{1}{v \times m(v_a - v_c)} \int I \, dV \text{ ---------- (3)}$$

In the formula, the range between (va-vc) represents the potential interval of the working electrode, v stands for the scan rate, m is the mass of the electro-active material $MgMn_2O_4$, and the total integral value of the CV curves are represented by I dV. Specific capacitance measurements for the $MgMn_2O_4$ electrode were 355, 299, 237, 187, 157, and 137 F g^{-1} for 5, 10, 25, 50, 75, and 100 mV s^{-1}, respectively.

To understand the electrochemical mechanism behind energy storage in the electrode material, the Dunn's technique was employed. This method provides a quantitative means to distinguish and determine the respective contributions to charge storage mechanisms at a specific potential, which include (i) surface capacitance effects and (ii) diffusion controlled insertion mechanism. The output current (I) at a specific potential (V) is the result of two distinct mechanisms, namely surface capacitive contribution (K1v) and diffusion-controlled faradic intercalation (K2v1/2), which depend on the scanning speed (v) and are quantifiable by the values K1 and K2.The current (i) derived through the Cyclic volumetric curve exhibits a power law relationship with the scan rate.

$$I = a\, v^{b} \text{ ---------- (4)}$$

The value of "b" can be found by doing slope analysis on the log i versus log v graph, as illustrated in Fig. 5(c).The slope of 0.5 indicates diffusion-controlled behaviours and a slope value of 1 suggests complete capacitive behaviour. The resulting b value of 0.6 shows that the $MgMn_2O_4$ electrodes displayed primarily diffusion-controlled behaviour with some capacitive behaviour. equation (5) can be utilized to quantitatively differentiate between the contributions of diffusion and capacitive mechanisms.

$$i(V) = K1v + K_2 v^{1/2} \text{ ---------- (5)}$$

Fig. 5(d) shows the percentage contribution of the diffusion and capacitive process for $MgMn_2O_4$ at different scan rates. The figure show redox reaction are more efficient at low scan rates than at higher scan rates. This may be because the reaction duration is longer at low scan rates. This indicates that as the scan rates increase, the Charge storage capability of an electrode through the diffusion-limited process decreases, resulting in a decrease in the specific capacitance of the electrode. Despite the 100 mVs-1 scan rate, the $MgMn_2O_4$ electrode still maintains capacity retention of approximately 38.9% (as shown in Fig. 5. (b)). This can be happened due to the distinctive nanorods shape of $MgMn_2O_4$.

CONCLUSION

To summarize, the synthesis of $MgMn_2O_4$ nano-rods was successfully prepared through co-precipitation using dual hydroxide treatments. The sample was thoroughly examined by PXRD, FTIR, SEM, and EDS. The electrode displayed excel-

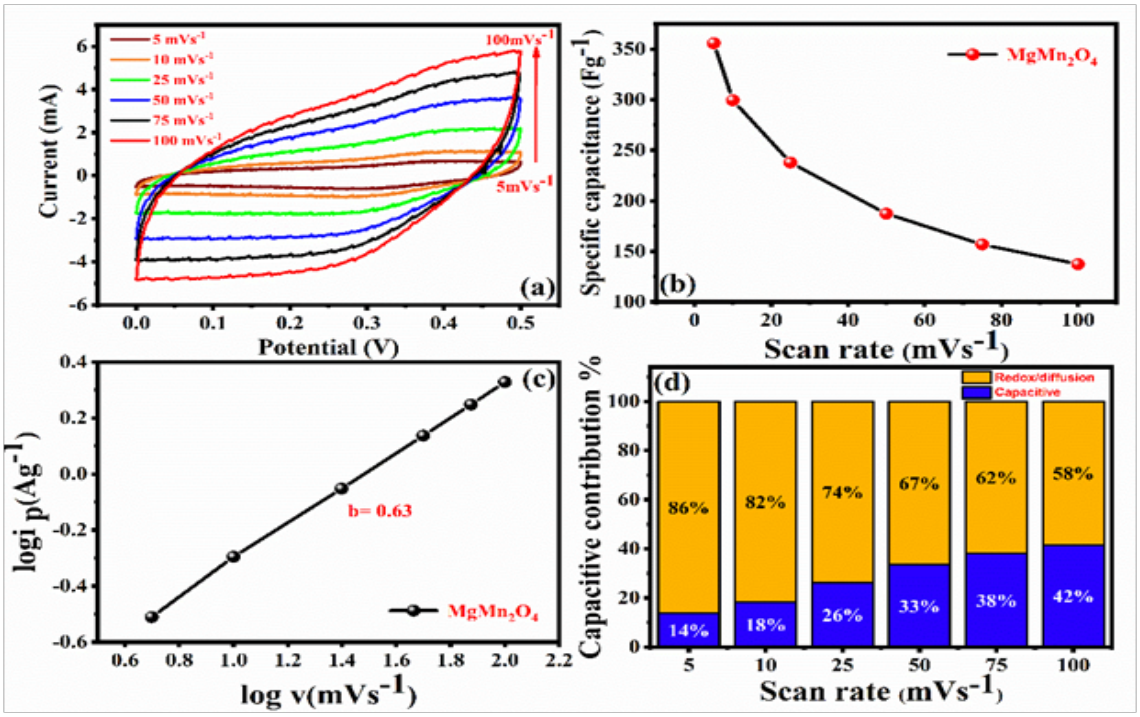

Fig. 5. (a)CVcurves of $MgMn_2O_4$(b) Correlation of scan rate and Specific CapacitanceVariations. (c) b-Value from Plot of logarithmic Scan Rate and logarithmic Anodic Peak Current (d) Percentage of redox and capacitive.

Table 1. Comparing MgMn2O4 Characteristics to Prior Research.

Electrode	Synthesis method	Cell configuration	Electrolyte	Capacitance(Fg-1)	Ref.
NiO	Hydrothermal method	3E	KOH	132 at 5 mVs-1	[6]
ZnO	Hydrothermal method	3E	KOH	178 at 2 mVs-1	[7]
WO_3	Electrodeposition method	3E	H_2SO_4	196 at 10 mVs-1	[8]
CuO	Reflux deposition	3E	[MOPMIM][Cl]	180 at 5 mVs-1	[9]
$CoMn_2O_4$	Electrospinning	3E	NaOH	121 at 5 mVs-1	[15]
$MgMn_2O_4$	Dual hydroxide treatment	3E	KOH	355 at 5 mV s-1	Present study

lent electrochemical characteristics with the highest specific capacitance of 355 Fg^{-1}at 5 mV s^{-1} scan rate in 6M KOH electrolyte. It was discovered that $MgMn_2O_4$'s distinctive nano-rod shape was the key to its improved electrochemical behaviour, providing enough of open space to store energy and improved its performance. Thus, the study highlights the potential of $MgMn_2O_4$ as a potential material for supercapacitor applications.

Reference

1. J. Bhagwan, B. N. V. Krishna, and J. S. Yu, "Template and sol-gel routed $CoMn_2O_4$ nanofibers for supercapacitor applications," no. April, pp. 11–15, 2021, doi: 10.1002/er.7096.
2. S. Suresh and V. Sindhu, "CeO_2/PANI/MoS^2 composite electrode for symmetric supercapacitor application," J. Indian Chem. Soc., vol. 99, no. 10, 2022, doi: 10.1016/j.jics.2022.100727.
3. V. Venkatachalam and R. Jayavel, "1D / 2D Co_3O_4 / Graphene Composite Electrodes for High-Performance Supercapacitor Applications," J. Electron. Mater., no. i, 2020, doi: 10.1007/s11664-020-08049-2.
4. M. Puratchimani, V. Venkatachalam, M. Rajapriya, and K. Thamizharasan, "Analytical & for Supercapacitor Applications," vol. 14, no. 10, pp. 968–979, 2022.
5. T. A. Sandosh and A. Simi, "Morphology controlled synthesis of one - dimensional $CoMn_2O_4$ nanorods for high - performance supercapacitor electrode application," Chem. Pap., vol. 75, no. 6, pp. 2295–2304, 2021, doi: 10.1007/s11696-020-01448-z.
6. S. D. Dhas et al., "Synthesis of NiO nanoparticles for supercapacitor application as an efficient electrode material," Vacuum, vol. 181, no. July, p. 109646, Nov. 2020, doi: 10.1016/j.vacuum.2020.109646.
7. I. Shaheen, K. S. Ahmad, C. Zequine, R. K. Gupta, A. G. Thomas, and M. A. Malik, "Facile ZnO-based nanomaterial and its fabrication as a supercapacitor electrode: synthesis, characterization and electrochemical studies," RSC Adv., vol. 11, no. 38, pp. 23374–23384, 2021, doi:

10.1039/D1RA04341B.

8. M. Qiu et al., "WO_3 nanoflowers with excellent pseudo-capacitive performance and the capacitance contribution analysis," J. Mater. Chem. A, vol. 4, no. 19, pp. 7266–7273, 2016, doi: 10.1039/c6ta00237d.
9. S. C. Bhise, D. V. Awale, M. M. Vadiyar, S. K. Patil, B. N. Kokare, and S. S. Kolekar, "Facile synthesis of CuO nanosheets as electrode for supercapacitor with long cyclic stability in novel methyl imidazole-based ionic liquid electrolyte," J. Solid State Electrochem., vol. 21, no. 9, pp. 2585–2591, 2017, doi: 10.1007/s10008-016-3490-2.
10. S. Selvarani, J. J. William, I. M. Babu, and G. Muralidharan, "One step synthesis of ZrO_2 microstructures for electrochemical capacitor applications," in AIP Conference Proceedings, 2019, vol. 2115, no. July, p. 030572. doi: 10.1063/1.5113411.
11. X. Gao et al., "Morphology-controllable preparation of $NiFe_2O_4$ as high performance electrode material for supercapacitor," Electrochim. Acta, vol. 296, pp. 181–189, 2019, doi: 10.1016/j.electacta.2018.11.054.
12. S. M. Nikam et al., "Pulsed laser deposited CoFe2O4thin films as supercapacitor electrodes," RSC Adv., vol. 10, no. 33, pp. 19353–19359, 2020, doi: 10.1039/d0ra02564j.
13. S. J. Uke, V. P. Akhare, D. R. Bambole, A. B. Bodade, and G. N. Chaudhary, "Cost effective synthesis of spinel $NiCo_2O_4$ nanocrystal by sol-gel citrate method and its application for supercapacitor," Int. J. Mater. Sci., vol. 12, no. 2, pp. 371–377, 2017, [Online]. Available: http://www.ripublication.com
14. J. Bhagwan, N. Kumar, and Y. Sharma, "Spinel-$MgMn_2O_4$ nanofibers: An attractive material for high performance aqueous symmetric supercapacitor," J. Energy Storage, vol. 46, no. December 2021, p. 103894, 2022, doi: 10.1016/j.est.2021.103894.
15. S. Alkhalaf et al., "Electrochemical Energy Storage Performance of Electrospun $CoMn_2O_4$ Nanofibers," J. Alloys Compd., vol. 692, pp. 59–66, 2016, doi: 10.1016/j.jallcom.2016.09.005.

How to cite this article:

Vijayamathubalan et al. (2026). Synthesis and Characterization of $MgMn_2O_4$ Nano-rods for Supercapacitor Electrode Applications. *Int J Recent Sci Res*.17(06), pp.722-727.

****